Low-Field Remanent Magnetization in the Weak Ferromagnet $Mn[N(CN)_2]_2$. Evidence for Spin-Flop Behavior

Jamie L. Manson,[1a,b] Carmen R. Kmety,[1c,d] Fernando Palacio*,[1e] Arthur J. Epstein*,[1c] and Joel S. Miller*,[1a]

Department of Chemistry, University of Utah, Salt Lake City, Utah 84112-0850, Department of Physics and Department of Chemistry, The Ohio State University, Columbus, Ohio 43210-1106, and Instituto de Ciencia de Materiales de Aragón, CSIC, Universidad de Zaragoza, 50009 Zaragoza, Spain

Received October 17, 2000. Revised Manuscript Received January 15, 2001

Low-field dc magnetization measurements have been performed on powder samples of the weak ferromagnet $Mn[N(CN)_2]_2$. In small dc fields, H ($0.01 \leq H \leq 100$ Oe), the zero-field and field-cooled magnetizations display the onset of a spontaneous moment below $T_c =$ 15.85(3) K, giving small magnetization values which suggest a spin-canted moment. A critical exponent, β, equal to 0.380(5) was obtained from a fit of the very low field remanent magnetization data to a power law. As the dc field is increased, the weak spontaneous magnetization continuously diminishes with respect to the total magnetization and the behavior typical of an antiferromagnet appears. When the field is increased, furthermore, a transition from the antiferromagnetic to a spin-flop state is observed.

Introduction

The occurrence of a spontaneous magnetization in a material is a characteristic typified by ferromagnets and is technologically very important. However, a spontaneous magnetization can also arise in magnetic systems possessing antiferromagnetic interactions as a result of several mechanisms.[2] Many researchers have enlisted the ferrimagnetic approach because two (or more) sublattices with dissimilar magnetizations exist. The highest T_c molecule-based magnets, $V(TCNE)_x \cdot yCH_2Cl_2$ ($T_c \sim 400$ K)[3a] and $V[Cr(CN)_6]_{0.86}$ ($T_c = 315$ K),[3b] take advantage of this paradigm. Other ferrimagnetic systems consisting of discrete molecules, one-dimensional chains, and/or two-dimensional layers have also been widely investigated and shown to magnetically order at low temperatures.[4] With this design principle, "crystal engineering" becomes useful, because materials with specified architectures and magnetic properties may be created.

Another origin for a spontaneous magnetization in an antiferromagnet arises when the antiparallel moments lack collinearity. Such canted antiferromagnetic systems also are called weak ferromagnets. For this phenomenon to take place, the system must undergo a transition to an essentially antiferromagnetically ordered state. As is often the case, magnetic ordering proceeds directly from the paramagnetic state. More complex behaviors such as spin reorientation, i.e., a transition from one magnetically ordered state to a different one, also can occur.

Spin canting can also occur in ferromagnetically coupled systems.[5] Two contributions are necessary for spin canting: (1) the presence of two nonsymmetry related nearest-neighbor magnetic ions and (2) and antisymmetric exchange and/or single-ion anisotropy.[2] Antisymmetric exchange is based solely upon symmetry arguments as shown by Dzyaloshinski,[6] while Moriya is credited with determining the mechanism by which individual spins interact via spin−orbit coupling and the relation between single-ion anisotropy and the magnitude of the interaction (vide infra).[7] Combination of the two arguments leads to the Dzyaloshinski−Moriya (DM) interaction. In the case of the second mechanism, the combined action of the different orientations of crystal fields acting at each site together with

(1) (a) University of Utah. (b) Present address: Chemistry and Materials Science Divisions, Argonne National Laboratory, 9700 S. Cass Ave., Argonne, IL 60439. (c) The Ohio State University. (d) Present address: Materials Science Division, Argonne National Laboratory, 9700 S. Cass Ave., Argonne, IL 60439. (e) CSIC, Universidad de Zaragoza.

(2) Palacio, F. *Mol. Cryst. Liq. Cryst.* **1997**, *305*, 385. Carlin, R. L. *Magnetochemistry*; Springer-Verlag: Berlin, 1986; p 206. Palacio, F. In *Localized and itinerant molecular magnetism. From molecular assemblies to the devices*; Coronado, E., Delhaes, P., Gatteschi, D., Miller, J. S., Eds.; NATO−ASI: Tenerife, 1995.

(3) Manriquez, J. M.; Yee, G. T.; McLean, R. S.; Epstein, A. J.; Miller, J. S. *Science* **1991**, *252*, 1415. (b) Ferlay, S.; Mallah, T.; Ouahes, R.; Veillet, P.; Verdaguer, M. *Nature* **1995**, *378*, 701. Hatlevik, O.; Buschman, W. E.; Zhang, J.; Manson, J. L.; Miller, J. S. *Adv. Mater.* **1999**, *11*, 914. Holmes, S. D.; Girolami, G. S. *J. Am. Chem. Soc.* **1999**, *121*, 5593.

(4) For example, see: (a) Decurtins, S.; Gross, M.; Schmalle, H. W.; Ferlay, S. *Inorg. Chem.* **1998**, *37*, 2443. (b) De Munno, G.; Poeria, T.; Julve, M.; Lloret, F.; Viau, G. *New J. Chem.* **1998**, 299. (c) Colacio, E.; Dominguez-Vera, J. M.; Ghazi, M.; Kivekäs, R.; Klinga, M.; Moreno, J. M. *Chem. Commun.* **1998**, 1071. (d) Pei, Y.; Verdaguer, M.; Kahn, O. *J. Am. Chem. Soc.* **1986**, *108*, 428.

(5) DeFotis, G. C.; Palacio, F.; O'Connors, C. J.; Bhati, S. N.; Carlin, R. L. *J. Am. Chem. Soc.* **1977**, *99*, 8314. (b) DeFotis, G. C.; Palacio, F.; Carlin, R. L. *Phys. Rev. B* **1979**, *20*, 2945. (c) Antorrena, G.; Palacio, F.; Ressouche, E.; Schweizer, J. *Physica B* **1997**, *234−236*, 780.

(6) Dzyaloshinski, J. *J. Phys. Chem. Solids* **1958**, *4*, 241.

(7) Moriya, T. *Phys. Rev.* **1960**, *120*, 91.

10.1021/cm0008314 CCC: $20.00
Published on Web 02/17/2001

the spin−orbit coupling leads to nonparallel directions of the magnetic anisotropy for each magnetic sublattice, respectively. In either mechanism the absence of a center of symmetry between interacting molecules is required. The general Hamiltonian used to describe symmetric exchange (spin−spin interaction) is $H = -2J\sum \mathbf{S}_i \cdot \mathbf{S}_j$, which does not permit canting of the spins and produces typical parallel or antiparallel alignment. The DM interaction is described by a term in the Hamiltonian given in eq 1, where $\mathbf{D}_{ij}$ is a constant

$$H_{\mathrm{DM}} = \mathbf{D}_{ij} \cdot [\mathbf{S}_i \times \mathbf{S}_j] \qquad (1)$$

vector. This interaction causes the spins to cant, thus reducing the coupling energy between $\mathbf{S}_i$ and $\mathbf{S}_j$. Because $\mathbf{D}_{ij}$ is proportional to $(g - 2)/g$, it is evident that, as g deviates appreciably from 2, the anisotropy is large and spin canting becomes increasingly important. The DM interaction is expected to be very small but not zero for the D_{4h} Mn^{II} in $Mn^{II}[N(CN)_2]_2$.

Regardless of the type of anisotropy, DM or single ion, it plays a significant role in the bulk magnetism of the material. Materials exhibiting weak to very strong magnetic anisotropy can exhibit spin canting. Some of the most well-known examples of spin-canted systems consist of nominally isotropic $S = {}^5/_2$ Mn^{II} or Fe^{III} cations,[8] although numerous other systems have been reported.[9] Note that spin canting may occur regardless of the lattice or spin dimensionality. Examples include zero-dimensional (molecular) $[FeCp_2][FeCl_4]$,[10] one-dimensional $CsCoCl_3 \cdot 2H_2O$,[11] two-dimensional $Cr[MePO_3] \cdot H_2O$,[12] and three-dimensional $[NH_4][MnF_3]$.[13] UCu_2Ge_2, an intermetallic, also possesses a canted ground state.[14]

Recently, we reported the results of magnetic[15a] and neutron[15b] studies carried out on $Mn[N(CN)_2]_2$ which clearly demonstrate a spin-canted ground state. Herein, we describe the temperature, $M(T)$, and field-dependent magnetization, $M(H)$, behaviors of $Mn^{II}[N(CN)_2]_2$ that show evidence for a field-induced phase transition to a spin-flop state.

Experimental Section

$Mn^{II}[N(CN)_2]_2$ was prepared as previously described.[15] dc magnetization measurements were carried out between 2 and 300 K, utilizing either a Quantum Design MPMS-5 or MPMS-5S SQUID magnetometers, with the latter equipped with a reciprocating sample operation (RSO) transport, enhanced low-temperature thermometry, and magnet reset ($H \leq \pm 2$ Oe). To perform low-field $M(T)$ experiments, the μ-metal shield was degaussed, the magnet reset, and a Hall probe utilized to null any residual magnetic field prior to sample insertion. Zero-field-cooled (ZFC) dc magnetization studies were taken by cooling in zero field to 2 K from 30 K and subsequently applying magnetic fields, H, of 0.01, 0.1, 1, 3, 5, 100, 500, 1000, 2000, 3500, 4500, 5000, 8000, and 10 000 Oe and data collected upon warming. Field-cooled (FC) dc magnetization measurements were obtained by cooling in an applied field from the highest measured temperature down to 2 K and data collected upon warming. Powdered samples of $Mn[N(CN)_2]_2$ weighing approximately 25−35 mg were loaded in gelatin capsules and mounted in plastic straws. All magnetic data were corrected for core diamagnetism as calculated from Pascal's constants, i.e., -72×10^{-6} emu/mol.

Results and Discussion

Three-coordinate dicyanamide, i.e., coordination of both nitrile N's and the central amide N to a paramagnetic transition metal, leads to weak ferromagnets and ferromagnets[15] with magnetic ordering temperatures as high as 47 K.[15a] In contrast, coordination of only the nitrile N's leads to weakly coupled antiferromagnets (in the case of Mn^{II} [16]). Examples where one nitrile N and the amide N are coordinated to a metal remain to be observed, although this structure has been postulated previously.[17] Three-dimensional framework structures are formed in the $M^{II}[N(CN)_2]_2$ (M = V, Cr, Mn, Fe, Co, Ni, Cu)[15,18,19,20] class of materials, where connectivities similar to rutile (TiO_2) are observed. The Cr and Mn examples possess weak ferromagnetic ground states due to spin canting below critical temperatures, T_c, of 47 and 16 K, respectively.

Because of short three-atom M←N≡C−N→M pathways, dicyanamide-based solids offer significantly enhanced magnetic properties relative to the tricyanomethanide-based materials,[16,21] which only have longer five-atom M←N≡C−N(→M)−C≡N→M exchange pathways. Interestingly, although strong antiferromagnetic interactions exist for $Cr^{II}[N(CN)_2]_2$, spin frustration does not occur, perhaps a consequence of the C_{2v} (as opposed to D_{3h}) symmetry of the $[N(CN)_2]^-$ ligand. In Chart 1, a

(8) For example, see: (a) Jirak, Z.; Salmon, R.; Fournes, L.; Menil, F.; Hagenmuller, P. *Inorg. Chem*. **1982**, *21*, 4218. (b) Battle, P. D.; Cheetham, A. K.; Long, G. J.; Longworth, G. *Inorg. Chem*. **1982**, *21*, 4223. (c) Mathonière, C.; Nuttall, C. J.; Carling, S. G.; Day, P. *Inorg. Chem*. **1996**, *35*, 1201. (d) Carling, S. G.; Day, P.; Visser, D. *Inorg. Chem*. **1995**, *34*, 3917.

(9) For example, see: (a) Mukherjee, S.; Ranganathan, R.; Roy, S. B. *Phys. Rev. B* **1994**, *50*, 1084. (b) Morón, M. C.; Palacio, F.; Clark, S. M.; Paduan-Filho, A. *Phys. Rev. B* **1995**, *51*, 8660. (c) Morón, M. C.; Palacio, F.; Rodríguez-Carvajal, J. *J. Phys.: Condens. Matter* **1993**, *5*, 4909. (d) Palacio, F.; Morón, M. C. In *Research Frontiers in Magnetochemistry*; O'Connor, C., Ed.; World Scientific Publishing: River Edge, NJ, 1993; p 227.

(10) Reiff, W. M.; Zhang, J. H.; Landee, C. P. *Solid State. Commun*. **1993**, *88*, 427.

(11) Herweijer, A.; de Jonge, W. J. M.; Botterman, A. C.; Bongaarts, A. L. M.; Cowen, J. A. *Phys. Rev. B* **1972**, *5*, 4618. (b) Kopinga, K.; van Vlimmeren, Q. A. G.; Bongaarts, A. L. M.; de Jonge, W. J. M. *Physica B* **1977**, *86*, 671.

(12) Bellitto, C.; Federici, F.; Ibrahim, S. A. *J. Chem. Soc., Chem. Commun*. **1996**, 759. (b) Bellitto, C.; Federici, F.; Ibrahim, S. A. *Chem. Mater*. **1998**, *10*, 1076

(13) Bartolomé, J.; Burriel, R.; Palacio, F.; González, D.; Navarro, R.; Rojo, J. A.; de Jongh, L. J. *Physica B* **1983**, *115*, 190. (b) Helmholdt, R. B.; Wiegers, G. A.; Bartolomé, J. *J. Phys. C* **1980**, *13*, 5081

(14) Chakravarti, A.; Ranganathan, R.; Roy, S. B. *Phys. Rev. B* **1992**, *46*, 6236.

(15) Manson, J. L.; Kmety, C. R.; Epstein, A. J.; Miller, J. S. *Inorg. Chem*. **1999**, *38*, 2552. (b) Kmety, C. R.; Huang, Q.; Lynn, J. W.; Erwin, R. W.; Manson, J. L.; McCall, S.; Crow, J. E.; Stevenson, K. L.; Miller, J. S.; Epstein, A. J. *Phys. Rev. B* **2000**, *62*, 5576.

(16) Manson, J. L.; Campana, C. F.; Miller, J. S. *Chem. Commun*. **1998**, 251.

(17) Mrozinski, J.; Hvastijova, M.; Kohout, J. *Polyhedron* **1992**, *11*, 2867.

(18) Kmety, C. R.; Manson, J. L.; Huang, Q.; Lynn, J. W.; Erwin, R.; Miller, J. S.; Epstein, A. J. *Mol. Cryst. Liq. Cryst*. **1999**, *334*, 605. (b) Kmety, C. R.; Manson, J. L.; Huang, Q.; Erwin, R. W.; Lynn, J. W.; Miller, J. S.; Epstein, A. J. *Phys. Rev. B* **1999**, *60*, 60.

(19) Batten, S. R.; Jensen, P.; Moubaraki, B.; Murray, K. S.; Robson, R. *Chem. Commun*. **1998**, 439. (b) Batten, S. R.; Jensen, P.; Kepert, C. J.; Kurmoo, M.; Moubaraki, B.; Murray, K. S.; Price, D. J. *J. Chem. Soc., Dalton Trans*. **1999**, 2987. (c) Murray, K. S.; Batten, S. R.; Moubaraki, B.; Price, D. J.; Robson, R. *Mol. Cryst. Liq. Cryst*. **1999**, *335*, 313. (d) Jensen, P.; Batten, S. R.; Fallon, G. D.; Moubaraki, B.; Murray, K. S.; Price, D. J. *Chem. Commun*. **1999**, 177.

(20) Kurmoo, M.; Kepert, C. J. *Mol. Cryst. Liq. Cryst*. **1999**, *334*, 693. (b) Kurmoo, M.; Kepert, C. J. *New J. Chem*. **1998**, *22*, 1515.

(21) Manson, J. L.; Ressouche, E.; Miller, J. S. *Inorg. Chem*. **2000**, *39*, 1135. (b) Manson, J. L.; Miller, J. S., unpublished results. (c) Batten, S. R.; Hoskins, B. F.; Moubaraki, B.; Murray, K. S.; Robson, R. *J. Chem. Soc., Dalton Trans*. **1999**, 2977.

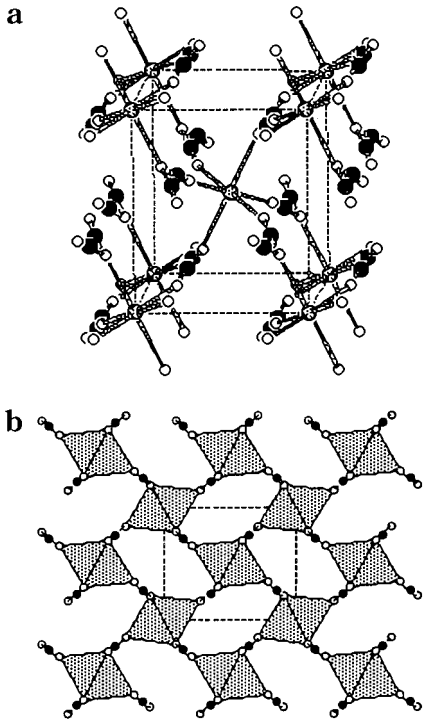

Figure 1. Unit cell of $Mn[N(CN)_2]_2$ showing the eight Mn nearest neighbors.[15b] Mn, C, and N atoms are depicted as shaded, filled, and open spheres, respectively, (a) Polyhedral representation of the crystal structure of $Mn[N(CN)_2]_2$. (b) C and N atoms are depicted as filled and open spheres, respectively.

Chart 1

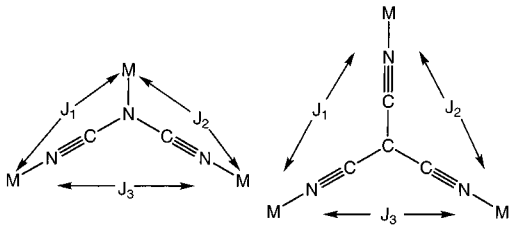

triangular array consisting of mostly isotropic paramagnetic metal centers is shown. In the case of $[C(CN)_3]^-$, each side of the triangle constitutes a J value, where $J_1 = J_2 = J_3$. This contrasts with $[N(CN)_2]^-$ bridging units, where two distinct J's coexist, i.e., $J_1 = J_2 \gg J_3$. Spin couplings via J_1 and J_2 (three atoms) are significantly stronger than that via J_3 (five atoms), affording antiferromagnetic interactions that are satisfied and not "frustrated" in the dicyanamide case.

The unit cell of $Mn[N(CN)_2]_2$ is shown in Figure 1a.[15b] Each metal center is octahedrally coordinated by six nitrogen atoms from six different $[N(CN)_2]^-$ ligands with local D_{4h} symmetry. Four of the six sites belong to equatorial nitrile nitrogens, and the two remaining axial sites are occupied by amide nitrogens to complete the coordination sphere. In turn, each $[N(CN)_2]^-$ is three-coordinate and adopts a trigonal bonding analogous to O^{2-} as found in TiO_2.[22] The basic structural unit of the three-dimensional network consists of one-dimensional ribbons, which extend along the c axis. In a single chain, the four dicyanamide nitrile nitrogens form a plane, i.e.,

(22) Wells, A. F. *Structural Inorganic Chemistry*, 5th ed.; Clarendon Press: Oxford, U.K., 1990, p 247.

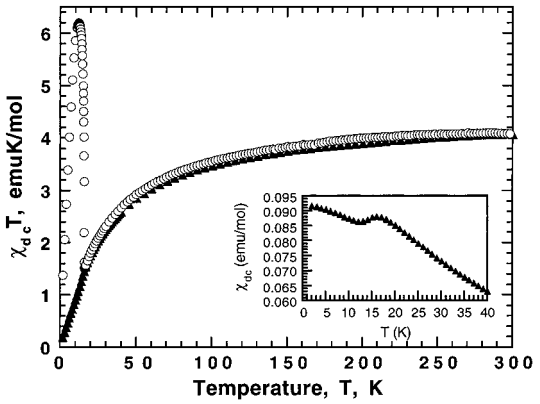

Figure 2. $\chi(T)$ taken upon warming in dc fields of 100 Oe (○) and 10 kOe (▲). $\chi(T)$ obtained at 10 kOe is shown in the inset.

MN_4, and because of the close proximity of neighboring chains, M bonding to the amide nitrogens of two additional $[N(CN)_2]^-$ ligands occurs. From analysis of the neutron powder diffraction data,[15b] at 4.2 K an elongated MnN_6 octahedron was observed with Mn−N≡C and Mn−$N(CN)_2$ distances of 2.181(2) and 2.302(2) Å, respectively. This result is in marked contrast to the bond distances found in $Mn[C(CN)_3]_2$, which are 2.222(1) and 2.272(2) Å.[21a] Furthermore, the N−Mn−N angles range from 85.4(1) to 94.6(1)°. Coordination of the nitrile nitrogen, N(1), to the Mn center affords a nonlinear angle of 158.9(2)° for Mn−N≡C. The resulting three-dimensional network lacks solvent, an unusual feature when interpenetrating lattices are not involved (Figure 1b). Furthermore, the closest Mn···Mn separation is 6.0854(2) Å [via Mn−N−C−N−Mn bonds]. The remaining close Mn···Mn separations are 6.1486(4), 7.3155(3), and 7.5371(2) Å and coincide with the a, b, and c unit cell parameters.

Temperature-Dependent Magnetic Properties. dc Magnetization. The magnetic susceptibility, $\chi(T)$, of $Mn[N(CN)_2]_2$, measured between 2 and 300 K was fit to the Curie−Weiss expression with $g = 2.00$ and $\theta = -16$ K ($T > 150$ K).[15a] The room temperature $\chi(T)$ value of 4.083 emu·K/mol is reduced from the spin-only value of 4.375 emu·K/mol expected for isolated $S = {}^5/_2$ ions in part due to the antiferromagnetic coupling of −16 K. Upon cooling, $\chi(T)$ constantly decreases as a result of antiferromagnetic short-range interactions. A sharp minimum in $\chi(T)$ is reached at 16 K followed by an abrupt increase. A maximum $\chi(T)$ value of 6.19 emu·K/mol was obtained at 12 K (T_{max}) in an 100 Oe applied field. This behavior is characteristic of weak ferromagnetism due to spin canting, affording a net magnetization. Below T_{max}, $\chi(T)$ decreases rapidly upon cooling further to 2 K. Furthermore, increasing H_{dc} to 10 kOe almost eliminates the peak in $\chi(T)$, giving behavior reminiscent of a typical antiferromagnet (Figure 2), and although previously reported,[15a] we include the $\chi(T)$ data acquired at 100 Oe for comparison. As shown in the inset of Figure 2, $\chi(T)$ lacks evidence of a spontaneous moment because the moment has been saturated in the field of 10 kOe and shows a rounded maximum centered near 16 K (0.088 emu/mol). Upon cooling further, $\chi(T)$ at 10 kOe decreases slightly, reaching a minimum value of 0.086 emu/mol at 12 K, and then increases smoothly to a value of 0.091 emu/mol at 2 K [Figure 2 (inset)].

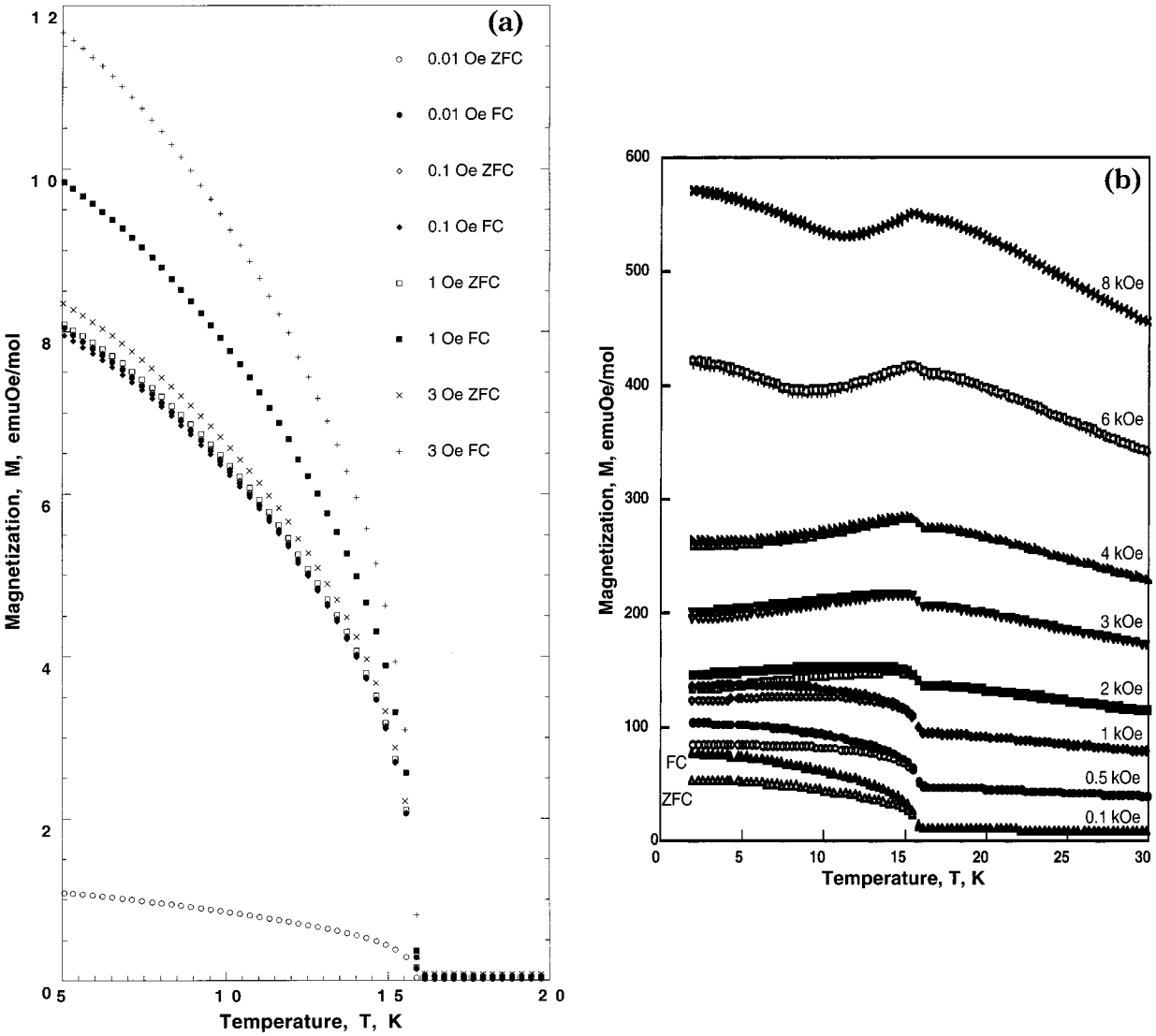

Figure 3. Zero-field and field-cooled magnetization data for Mn[N(CN)$_2$]$_2$ taken in (a) ultralow fields and (b) larger dc fields between 0.1 and 10 kOe.

Zero-field and field-cooled magnetization measurements in several applied dc fields provide a clear indication of the uncompensated moment for Mn[N(CN)$_2$]$_2$ below a magnetic ordering temperature of 16 K (Figure 3). For all fields (H) measured, the bifurcation temperature, T_b, is independent of the applied field, indicating the lack of spin glass behavior.[23] As H is increased, it appears that the zero-field and field-cooled curves gradually collapse together; i.e., the weak ferromagnetic moment becomes saturated. Also note that above T_c the magnetization becomes increasingly nonzero, because of the contribution of the χH term. The spontaneous moment, albeit weak, continuously diminishes with respect to the total magnetization up to the highest field measured (10 kOe) with increasing applied dc field. Fitting of the 0.01 Oe remanent magnetization, $M_r(T)$, data to a power law, $M_r \propto (T - T_c)^{\beta}$ (Figure 4), yielded $T_c = 15.85(3)$ K and $\beta = 0.380(5)$, which is in accord with the value anticipated (0.37) for an isotropic three-dimensional Heisenberg system.[24]

The variable-temperature behavior of Mn[N(CN)$_2$]$_2$ is similar to that of several other $S = {}^5/_2$ Mn^{II} materials, especially perovskite-like [NH$_4$][MnF$_3$],[13] which antiferromagnetically orders ($T_N = 75.1$ K) with a small net moment. The small ferromagnetic component was manifested as an anomaly in the magnetic susceptibility, $\chi(T)$, in small applied fields. At T_N there is an abrupt increase in $\chi(T)$, likely induced by spin canting between the two magnetic sublattices. In a neutron scattering study of [NH$_4$][MnF$_3$], an attempt was made to elucidate the spin-canting angle. Although no evidence of an uncompensated moment was detected via neutron diffraction, a canting angle of $<1°$ could explain the observed magnetic behavior.[13b] The canting angle for Mn[N(CN)$_2$]$_2$ is $<5°$ with respect to the a axis in the ab plane from powder neutron diffraction studies.[15b] An independent measure of the canting angle was estimated by extrapolation of the $M(H)$ data to $H = 0$ [Figure 5(inset)], using low-field ($H < 4$ kOe) data yielding 0.05°, in agreement with an estimate reported in ref 20b.

Field-Dependent Magnetic Properties. Similar to [NH$_4$][MnF$_3$], upon measuring the temperature-depend-

(23) Mydosh, J. A. *Spin Glasses*; Francois and Taylor: Washington, DC, 1993

(24) de Jongh, L. J.; Miedema, A. R. *Adv. Phys.* **1974**, *23*, 1.

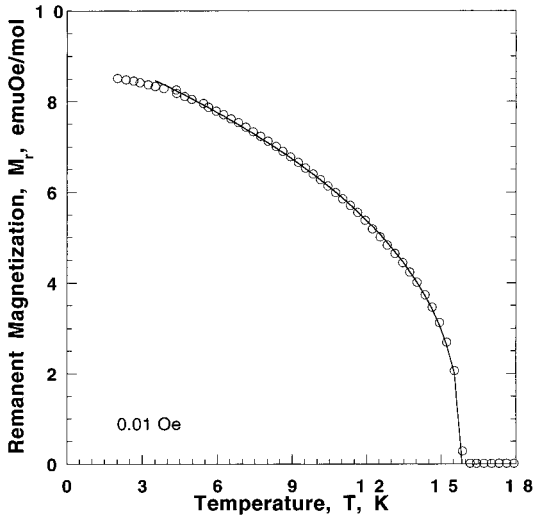

Figure 4. Remanent magnetization of 0.01 Oe (○) and a fit to a power law (—): $M_r(T) = a[T_c - T]^{\beta}$ with $a = 3.17(4)$ emu·Oe/K·mol, $T_c = 15.85(3)$ K, and $\beta = 0.380(5)$. The Heisenberg model predicts $\beta = 0.37$, and the Ising model predicts $\beta = 0.31$.

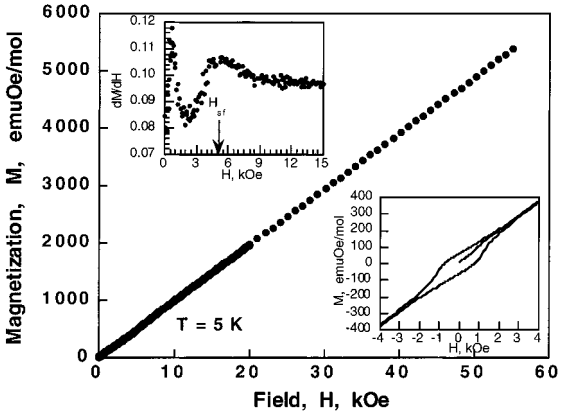

Figure 5. Isothermal magnetization of 5 K, $M(H)$, and dM/dH (inset) data for $Mn[N(CN)_2]_2$. The second inset is the hysteresis loop for $Mn[N(CN)_2]_2$ also at 5 K.

ent susceptibility in a static dc field of 10 kOe for $Mn[N(CN)_2]_2$, the weak ferromagnetic peak in $\chi(T)$ vanished (Figure 2) and the powder-averaged $\chi_\perp(T)$ result was obtained as expected; i.e., a simple spin-flopped two-lattice antiferromagnet appeared. The magnetic susceptibility data of $Mn[N(CN)_2]_2$ and $[NH_4][MnF_3]$ are very similar and, in fact, yield analogous behavior when $H = 10$ kOe. Isothermal magnetization at 5 K revealed behavior associated with a canted antiferromagnet below T_N (Figure 5). The magnetization rises nearly linearly to the highest field measured of 5 T, although a slight inflection was observed near 5000 Oe. At 5.5 T a low magnetization value of 5400 emu·Oe/mol was obtained, i.e., only ~20% of the expected value of 27 900 emu·Oe/mol for $S = {}^5/_2$ ions, which is consistent with antiferromagnetic ordering. A hysteresis loop consistent with a weak ferromagnet was found for $Mn[N(CN)_2]_2$, with a coercive field, H_{cr}, of 750 Oe and $M_r = 63$ emu·Oe/mol [Figure 5 (inset)]. The calculated derivative of the magnetization, $\partial M/\partial H$, shows a discontinuity at ~0.8 kOe, a second peak at 5.0 kOe, and zero slope upon increasing H [Figure 5 (inset)]. The peak at 5.0 kOe is attributed to an antiferromagnetic to spin-flop (SF) transition, which occurs when the antiparallel spin

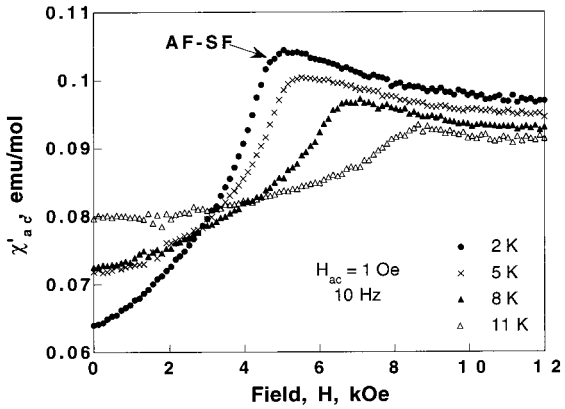

Figure 6. $\chi'(H)$ for $Mn[N(CN)_2]_2$ taken at 2, 5, 8, and 11 K.

alignment (AF) "flops" perpendicular to the applied magnetic field. To confirm these findings, the ac susceptibility as a function of the field, $\chi'(H)$, was measured at 2 K using a 10 Hz oscillating field of 1 Oe. The 5.0 kOe peak was reproduced, while the 0.8 kOe peak was not. Presently, the origin of the 0.8 kOe peak is unclear and may be due to some unforeseen artifact. Additional measurements at 5, 8, and 11 K show the temperature dependence of the spin-flop field; H_{sf} increases as the temperature increases, i.e., 5.5, 7.0, and 8.6 kOe, respectively (Figure 6). As the applied field increases, at some point on the H/T phase diagram (vide infra), there should also be a spin-flop to paramagnetic phase transition at H_c, where the magnetization of the two antiferromagnetically interacting sublattices are forced to be parallel by the magnetic field. For $Mn[N(CN)_2]_2$ this field has been observed at ~130 kOe at 0.037 K,[15b,25] much higher than that the observed for $Mn[N(CN)_2]_2$-(pyrazine) at 28.3 kOe.[26]

The temperature dependence of the spin-flop (SF) field can be linearly extrapolated to $T = 0$ K to obtain $H_{SF}(T{=}0) = 4.8$ kOe. Using the mean-field relations[2,13a]

$$H_{SF}(0) = [2H_E H_A - H_A{}^2]^{1/2}$$

$$H_c(0) = 2H_E - H_A$$

where H_E and H_A are respectively the exchange and anisotropy fields, and taking the observed value of H_c at $T = 0.037$ K, $H_c(0)$, one obtains $H_A = 0.18$ kOe and $H_E = 65$ kOe. The anisotropy constant $\alpha = H_A/H_E$ is $\sim 2 \times 10^{-3}$ for this compound. The low value of this anisotropy constant compares well with other values found in related $S = {}^5/_2$ Heisenberg antiferromagnets as shown in Table 1.

Magnetic Phase Diagram. The H vs T phase diagram for polycrystalline $Mn[N(CN)_2]_2$ is shown in Figure 7. The AFM−SF boundary was determined from the maxima of the peak in the $\chi'(H)$ data (i.e., Figure 6), while the AFM−PM boundary was obtained from the $M(T)$ data (i.e., Figure 3). At temperatures well below the bicritical temperature (T_b), H_{SF} is well-defined while the maximum in $\chi'(H)$ broadens as T_N is approached

(25) Kmety, C. R.; Manson, J. L.; Huang, Q.; Lynn, J. W.; Erwin, R.; McCall, S.; Crow, J. E.; Stevenson, K. L.; Miller, J. S.; Epstein, A. J., in preparation.

(26) Manson, J. L.; Incarvito, C. D.; Rheingold, A. L.; Miller, J. S. *J. Chem. Soc., Dalton Trans.* **1998**, 3705.

Table 1. Magnetic Phase Diagram Characteristics of Representative $S = {}^5/_2$ Heisenberg Antiferromagnets

compound	T_c (K)	$H_{SF}(0)$(kOe)	$H(0)$ (kOe)	$H_E(0)$(kOe)	α	ref
$Cs_2[Fe^{III}Cl_5]\cdot H_2O$	6.54	11.5	0.88	75.9	12×10^{-3}	*a*, *b*
$Rb_2[Fe^{III}Cl_5]\cdot H_2O$	10.00	14.3	0.59	172.4	3.4×10^{-3}	*b*, *c*
$K_2[Fe^{III}Cl_5]\cdot H_2O$	14.06	27.0	1.7	199.4	8.5×10^{-3}	*b*, *d*
NH_4MnF_3	75.1	3.7	0.140	116.7	1.2×10^{-3}	13a
$(MeNH_3)MnCl_3\cdot 2H_2O$	4.12	19	0.85	212.5	4×10^{-3}	*e*
$MnC_4H_4O_6\cdot 2H_2O$	1.83	4.8	0.6	19.4	31×10^{-3}	*f*
$Mn[N(CN)_2]_2$	15.85	4.8	0.18	65	2×10^{-3}	this work, 15b, 25

[a] Paduan-Filho, A.; Palacio, F.; Carlin, R. L. *J. Phys (Paris)* **1978**, *39*, L-279. [b] Carlin R. L.; Palacio, F. *Coord. Chem Rev.* **1985**, *65*, 141. [c] Campo, J.; Palacio, F.; Morón, M. C.; Becerra, C. C.; Paduan-Filho, A. *J. Phys.*: *Condens. Matter* **1999**, *11*, 4409. [d] Palacio, F.; Paduan-Filho, A.; Carlin, R. L. *Phys. Rev. B* **1980**, *21*, 296. [e] Paduan-Filho, A.; Oliveira, N. F., Jr. *J. Phys. C* **1984**, *17*, L859. [f] Paduan-Filho, A.; Becerra, C. C. *J. Phys.*: *Condens. Matter* **2000**, *12*, 2071.

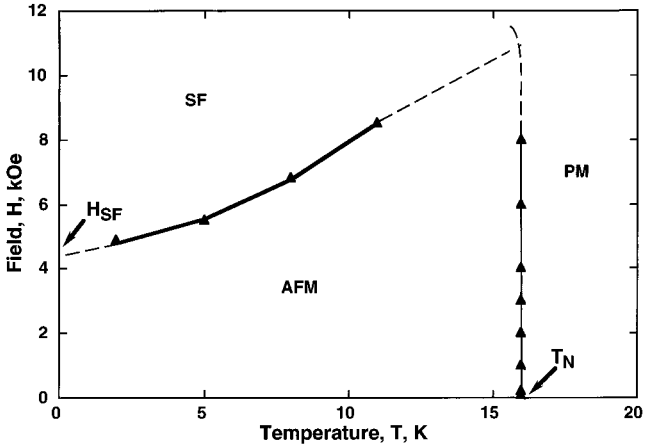

Figure 7. $H(T)$ phase diagram for $Mn[N(CN)_2]_2$. AFM = antiferromagnetic, SF = spin flop, and PM = paramagnetic. The solid and dashed lines serve only as guides for the eyes.

from the low-temperature regime, as expected. For example, in the diagram below approximately 5 K, H_{SF} remains essentially invariant. Increasing the temperature beyond 5 K results in a significant increase and broadening of H_{SF}. In this diagram, we have not included the SF−PM boundary nor the millikelvin region along the AFM−SF boundary. This work will be reported elsewhere.[25] From these studies it will be possible to complete the SF−PM boundary and elucidate the bicritical point.

Conclusion

Rutile-like $Mn^{II}[N(CN)_2]_2$ behaves as a weak ferromagnet which exhibits a spontaneous magnetization in a wide range of applied dc magnetic fields below T_c = 15.85(3) K. Isothermal magnetization measurements conducted at low temperature show hysteresis with H_{cr} = 750 Oe and M_r = 63 emu·Oe/mol (5 K). Magnetic measurements as a function of the field display the onset of a spin-flop phase transition from the antiferromagnetic state. At 2 K the critical field for the spin-flop transition, H_{SF}, is observed at 5.0 kOe, which shifts to 5.5 kOe (5 K), 7.0 kOe (8 K), and 8.6 kOe (11 K). No evidence for the spin-flop to paramagnetic phase transition was detected up to 55 kOe. Ultralow-field dc measurements (<3 Oe) were made and shown to differ only by a scale factor, for data obtained up to 100 Oe. The spin-canting angle was estimated to be ∼0.05° from the 5 K $M(H)$ at low fields in agreement with an earlier estimate.[20b]

Acknowledgment. The authors gratefully acknowledge the U.S. Department of Energy (Grants DE-FG03-93ER45504 and DE-FG02-86ER45271), National Science Foundation (Grant DMR95-01325), the American Chemical Society Petroleum Research Fund (Grant 30722-AC5), and the Comisión Interministerial de Ciencia y Tecnología (Grant MAT97-0951) for support of this work.

CM0008314